This paper was prepared by a USDA employee as part of the employee's official duties and cannot legally be copyrighted. The fact that the private publication in which the paper may appear is itself copyrighted does not affect the material of the U.S. Government, which can be reproduced by the public at will.

Journal of Hydrology 229 (2000) 149-167

Estimating parameters for a dual-porosity model to describe nonequilbrium, reactive transport in a fine-textured soil

R.C. Schwartz[a,*], A.S.R. Juo[b], and K.J. McInnes[b]

[a]*USDA-ARS, P.O. Drawer 10, Bushland, TX 79012, USA*
[b]*Department of Soil and Crop Sciences, Texas A&M University, College Station, TX 77843, USA*

Received 30 March 1999; received in revised form 16 November 1999; accepted 23 December 1999

Abstract

Several models have recently been proposed to describe solute transport in two or more mobile regions, yet there have been relatively few attempts to calibrate these models for a particular soil. In this study, a dual-porosity approach is used to describe the steady-state reactive transport of a Br^- tracer through a fine-textured Ultisol over a range of pore water velocities and levels of soil water saturation. This model partitions the soil into two mobile regions that represent the soil matrix and macropores. Theory and methodology are presented to estimate dispersive transport and adsorption in each region and diffusive exchange between regions for soil columns subjected to steady-state water flow. Numerical inversion of the governing transport equations was used in conjunction with nonlinear least-squares optimization to estimate transport parameters for displacement experiments. Pore water velocity and water content was independently estimated for each region using a pair of displacement experiments conducted on the same column but at different degrees of saturation. Results suggest that the fitted mass exchange coefficient represents a lumped process resulting from the combined effects of intra-aggregate diffusion and local flow variations. We also conclude that when there is limited interaction between regions, the mass transfer coefficient should be estimated independently. A principal difficulty of the application of the dual-porosity model was the nonlinear behavior of the diffusive exchange term at early times after a step change in inlet concentration. Another problem was that fitted solutions predicted nearly all adsorption sites to be in equilibrium with solute in the macropore region rather than with solute in the matrix region. Despite these difficulties, the dual-porosity model led to differentiation of transport processes that corresponded to observed structural differences in soil horizons.

Keywords: Solute transport; Inverse parameter estimation; Two-region model; Diffusive exchange

1. Introduction

Soils often exhibit a variety of small scale heterogeneities such as cracks, macropores and voids which permeate and separate the matrix or inter-aggregate pore regions. A consequence of the wide variations in fluid velocity generated by heterogeneous void space within an averaging volume is that the transport processes in some soils and geologic formations cannot be successfully described using the advective-dispersive equation (ADE). A common approach to deal with these difficulties is to partition flow into two or more regions based upon the pore size. Early proponents of a dual-porosity approach (Barenblatt et al.,1960; Warren and Root, 1963) hypothesized that such a concept was useful to describe water transport in fractured porous media. The dual-porosity approach consists of the introduction of a liquid pressure and mean velocity for each of the pore size groupings. Continuum equations of fluid and solute mass conservation are written separately for each pore size class and inter-region advective and diffusive

* Corresponding author. Fax: + 806-356-5750.
E-mail address: rschwart@ag.gov (R.C. Schwartz)

exchange terms provide for the interaction between groupings.

A host of models have been introduced to overcome the difficulties of describing solute transport in soils which exhibit exceedingly wide distributions in pore water velocities. Stagnant region models (Coats and Smith, 1964; van Genuchten and Wierenga, 1976) partition liquid into mobile and immobile regions with solute exchanges being a function of concentration differences. Although mobile-immobile models have been the most successful in describing solute transport in soil columns, they suffer from the fact that the immobile fraction is operationally defined and fitted parameters change as a function of experimental conditions. Skopp et al. (1981) introduced a dual-porosity model for solute transport in soils whereby both regions are mobile and solute exchange occurs between the regions. However, convergent approximations of analytical solutions could not be obtained for relatively large exchange coefficients. More recently Gerke and van Genuchten (1993a) and Ray et al. (1997) introduced a dual-porosity model which accounts for both advective and diffusive exchanges of solute under non-steady-state flow conditions. Expanding the concept, Gwo et al. (1995) used three pore regions to describe water and solute transport under variably saturated conditions. Exchange of solutes between pore groups was governed by advective and diffusive exchange coefficients between the three regions.

Despite a modest number of dual and multi-porosity models in the literature that have been used to describe unsaturated transport of solutes in structured soils (e.g. Skopp et al, 1981; Gerke and van Genuchten, 1993a; Gwo et al., 1995; Hutson and Wagenet, 1995; Ray et al., 1996) there have been few attempts to calibrate or validate these models. Ma and Selim (1995) used a two-region model to describe tritium transport in *repacked* soil columns. The flux in each region and a single dispersivity for both regions were obtained by best fit procedures. They found that the use of the two-region model could describe the bimodal peaks of breakthrough curves generated with pulse inputs of tritium. However, a constant diffusive exchange coefficient was assumed for all experiments because attempts to fit the exchange coefficient concurrently with other parameters were unsuccessful. Gwo et al. (1995) fitted a three-region model to effluent concentrations obtained from displacement experiments for a single undisturbed soil column. The model was fitted to three breakthrough curves obtained from displacements conducted at different pressure heads (i.e. 0, -10, and -15 cm H_2O). Since the experiments were conducted under steady-state flow, it was assumed that there was no advective exchange of solute. This permitted the estimation of the three diffusive solute exchange coefficients between the three regions. However, since eight additional parameters were fitted to each displacement experiment, it is questionable if the solution is unique and if fitted model parameters actually reflect the effective transport processes in the soil. These above noted difficulties exemplify the inherent problems associated with obtaining reliable estimates of effective transport parameters for each pore region when independently measured estimates are not obtainable. Nonetheless, it is essential to evaluate the degree to which multi-continuum models correctly predict experimental data.

This research was conducted in southern Costa Rica and was part of a larger study investigating the physical and chemical mechanisms governing the transport of tracers in a variable charge soil. Both physical nonequilibrium and anion adsorption were considered to be potentially important processes controlling the movement of nitrate in soils of this region which receives approximately 3000 mm precipitation annually. In this study, the dual-porosity approach is evaluated with respect to its utility in describing the steady-state reactive transport of a Br^- tracer through large, undisturbed soil columns at different soil water contents and pore water velocities. Only two mobile regions are considered to reduce the difficulties associated with nonuniqueness when attempting to estimate multiple mass transfer coefficients between three or more regions. Theory and methodology are presented to estimate diffusive exchange and transport parameters for a soil column at a given water flux using nonlinear least-squares regression in conjunction with data obtained from a displacement experiment conducted at a lower pressure head and slower pore water velocity. Model performance is evaluated by comparing simulated concentrations with experimental measurements and by discerning the degree to which fitted parameters vary in a meaningful manner as physical and chemical conditions of the experiments change.

2. Theory

2.1. Governing equations

For one-dimensional, incompressible flow with negligible density effects due to concentration gradients, solute transport in each region can be described using the ADE

$$\frac{\partial(\theta_1 C_1)}{\partial t} + \frac{\partial(f \rho_b S_1)}{\partial t} = \frac{\partial}{\partial x}\left(D_1 \theta_1 \frac{\partial C_1}{\partial x} - v_1 \theta_1 C_1\right) - \Gamma \quad (1)$$

$$\frac{\partial(\theta_2 C_2)}{\partial t} + \frac{\partial[(1-f) \rho_b S_2]}{\partial t} = \frac{\partial}{\partial x}\left(D_2 \theta_2 \frac{\partial C_2}{\partial x} - v_2 \theta_2 C_2\right) + \Gamma \quad (2)$$

where subscript 1 represents the macropore or inter-aggregate pore region and subscript 2 represents the soil matrix or intra-aggregate pore region. The variables C_1 and C_2 are resident solute concentrations corresponding to solute mass per unit volume of water in each respective pore group (M L^{-3}) and S_1 and S_2 are adsorbed mass of solute per unit of soil mass that equilibrates with the solution contained in each respective region (M M^{-1}). Here ρ_b is the bulk density of the soil (M L^{-3}), f is the mass fraction of soil that equilibrates with the solution in region 1 with respect to total soil mass (M M^{-1}), θ_1 and θ_2 are the volumetric water contents of each respective region per unit soil volume (L^3 L^{-3}), v_1 and v_2 are the pore water velocities for each respective pore region (L T^{-1}), D_1 and D_2 are the longitudinal dispersion coefficients for each respective region (L^2 T^{-1}), x is distance in the direction of flow (L), t is time (T), and Γ is the net solute exchange rate per unit soil volume per unit time (M L^{-3} T^{-1}).

The exchange term Γ is comprised of both advective and dispersive transfers. Barenblatt et al. (1960) hypothesized that the volume transfer of liquid between pore groups is dependent upon the pressure drop between regions, the liquid viscosity, and the geometrical characteristics of the medium. Thus, as might be expected, the advective solute exchange rate is a function of an effective hydraulic conductivity multiplied by the pressure drop. Dispersive mixing between regions can be modeled in the likeness of mixing between two tanks. Let ε represent the rate of mixing expressed as the pore volumes of θ_1 mixed with an equivalent number of pore volumes from θ_2 per unit time interval. The same volume removed from each region is returned, but with a different concentration. This conceptualization allows the derivation of the linear diffusive mass exchange term (Schwartz, 1998). The net solute exchange rate including both advective and diffusive transfers is therefore

$$\Gamma = K_{1,2}(\theta_{1,2}) \Lambda (h_1 - h_2) C_{1,2} + \varepsilon \frac{\theta_1 \theta_2}{\theta_1 + \theta_2}(C_1 - C_2) \quad (3)$$

where $K_{1,2}(\theta_{1,2})$ is the effective hydraulic conductivity between regions (L T^{-1}), h_1 and h_2 are the pressure heads associated with each respective pore group (L), Λ is the fluid exchange coefficient (L^{-2}) between regions, and ε is the solute diffusive exchange coefficient between regions (T^{-1}). Here $C_{1,2}$ is the resident solute concentration (M L^{-3}) that depends upon the direction of flow (Gerke and van Genuchten, 1993a).

For a linearly exchanging solute, an adsorbed phase that equilibrates instantaneously with the solution phase, and assuming that exchange sites are distributed randomly throughout the media, adsorbed concentrations in each region can be defined as

$$S_1 = K_d C_1 \quad (4)$$

$$S_2 = K_d C_2 \quad (5)$$

where K_d is the distribution coefficient (L^3 M^{-1}). Assuming that soil properties do not vary substantially with depth, a unit hydraulic gradient implies that $h_1 = h_2$ and transfers between regions generated by gradients in pressure head should be negligible. Combining this assumption with Eq. (1) through (3) and substituting the time derivatives of Eqs. (4) and (5) in for $\partial S_1/\partial t$ and $\partial S_2/\partial t$ yields the following coupled partial differential equations for steady-state transport

$$R_1 \frac{\partial c_1}{\partial t} = D_1 \frac{\partial^2 c_1}{\partial x^2} - v_1 \frac{\partial c_1}{\partial x} - \varepsilon \frac{\theta_2}{\theta_1 + \theta_2}(c_1 - c_2) \quad (6)$$

$$R_2 \frac{\partial c_2}{\partial t} = D_2 \frac{\partial^2 c_2}{\partial x^2} - v_2 \frac{\partial c_2}{\partial x} + \varepsilon \frac{\theta_1}{\theta_1 + \theta_2}(c_1 - c_2) \quad (7)$$

where R_1 and R_2 are the dimensionless retardation

factors for each region and defined as

$$R_1 = 1 + \frac{f \rho_b K_d}{\theta_1} \quad (8)$$

$$R_2 = 1 + \frac{(1 - f) \rho_b K_d}{\theta_2} \quad (9)$$

and c_1 and c_2 are the dimensionless resident concentrations specified as

$$c_1(x,t) = \frac{C_1(x,t) - C_i}{C_0 - C_i} \quad (10)$$

$$c_2(x,t) = \frac{C_2(x,t) - C_i}{C_0 - C_i} \quad (11)$$

where C_i is the initial uniform concentration at $t = 0$ and C_0 is the concentration in the entrance reservoir.

The coupled partial differential equations were solved subject to the following initial conditions (12a) and (12b) and boundary conditions (12c) through (12f)

$$c_1(x,0) = 0 \quad (12a)$$

$$c_2(x,0) = 0 \quad (12b)$$

$$\lim_{x \to 0^+} \left[c_1(x,t) - \frac{D_1}{v_1} \frac{\partial c_1(x,t)}{\partial x} \right] = 1 \quad (12c)$$

$$\lim_{x \to 0^+} \left[c_2(x,t) - \frac{D_2}{v_2} \frac{\partial c_2(x,t)}{\partial x} \right] = 1 \quad (12d)$$

$$\lim_{x \to \infty} \frac{\partial c_1(x,t)}{\partial x} = 0 \quad (12e)$$

$$\lim_{x \to \infty} \frac{\partial c_2(x,t)}{\partial x} = 0 \quad (12f)$$

In contrast to other dual-porosity or multi-continuum solute transport models which utilize a finite lower boundary condition (e.g. Gerke and van Genuchten, 1993a; Gwo et al., 1995; Ma and Selim, 1995; Ray et al., 1997) the solutions obtained in this study are formulated using Neumann lower boundary conditions at an effectively infinite distance from the inlet. At low Péclet numbers, the use of an infinite boundary condition was found to provide a better description of column effluent concentrations because axial variations in velocity were principally responsible for dispersion rather than molecular diffusion (Schwartz et al., 1999). Moreover, use of an infinite lower boundary condition permits a direct comparison of the two-region solution with the one-region ADE solution of Lapidus and Amundson (1952) and the mobile-immobile region model (Parker and van Genuchten, 1984b) typically employed to analyze miscible displacement experiments.

2.2. Experimental approach of parameter estimation

In many structured soils, the ADE has been found to provide an accurate description of solute transport at slow pore water velocities corresponding to unsaturated conditions at relatively low (i.e. 10 to 20 cm H_2O) tensions (Elrick and French, 1966; Seyfried and Rao, 1987; Jardine et al., 1993). As saturation increases, however, the manner in which solutes are transported in these soils diverges from that predicted by the ADE. It has been hypothesized that the increasingly better description provided by the ADE as tension increases reflects the removal of the contribution of macropores towards total mass flux (Jardine et al., 1993). Therefore, the macropore region can be operationally defined as that portion of the pore space that when active during steady-state flow conditions, yields asymmetrical breakthrough curves not corresponding to Fickian dispersion theory. Let h_{eq} be the pressure head that corresponds to the volumetric moisture content θ_2 at which the matrix region is saturated during steady-state flow. Additionally, θ_1 is the volume of water that resides in macropores or inter-aggregate pore space during steady-state flow conditions. The volumetric water content of the bulk soil is given by $\theta = \theta_1 + \theta_2$. Accordingly, by the previous definition of the macropore region, breakthrough curves obtained from displacement experiments conducted at pressure heads greater than h_{eq} will exhibit asymmetrical behavior. At these pressure heads the steady-state dual-porosity model Eq. (6) and (7) can be employed to describe solute transport in each region delimited by the

volumetric water contents $\theta_1$and θ_2. In this manner, a series of column displacement experiments can be conducted at a several pressure heads ranging from h_{eq} to zero to permit the calibration of the dual-porosity model to a particular soil column. The advantage of operationally defining the volumetric water content of the macropore region instead of obtaining an estimate through fitting procedures (e.g. Gwo et al., 1995; Ma and Selim, 1995) are that a mean pore water velocity and water flux can be identified with each region.

Let D and R represent the dispersion coefficient and retardation factor obtained from the fit of the one-region ADE to a column displacement experiment conducted at a pressure head of h_{eq}. At pressure heads of h_{eq}, all of the surface area associated with Br^- exchange is assumed to be active even though the soil is not saturated. This is a reasonable approximation since at these low tensions, large pores would be empty yet the walls of these pores would still be wetted by the soil solution and hence be able to participate in exchange. Consequently, the expected equilibrium retardation factor R_{eq} for the entire soil volume at a moisture content θ greater than θ_2 is therefore

$$R_{eq}(\theta) = 1 + \frac{\rho_b K_d}{\theta} = 1 + \frac{\theta_2}{\theta}\cdot\left[R(\theta_2) - 1\right] \quad (13)$$

Combining Eq. (8), (9) and (13) yields the following expression for the retardation factor in the matrix region

$$R_2 = 1 + \left[R_{eq}(\theta) - 1\right]\cdot\frac{\theta}{\theta_2} - \left[R_1 - 1\right]\cdot\frac{\theta_1}{\theta_2} \quad (14)$$

Thus, in Eq. (6) and (7) only R_1 need be fitted to obtain estimates of R_2 and f, the fraction of adsorption sites that equilibrate with the solution in the macropore region. As a result of incorporating information from two displacement experiments into the dual-porosity model, the number of unknowns in the dual-porosity model is reduced to four parameters. In addition, some of the uncertainty involved in evaluating f and the effectively immobile water content associated with the mobile-immobile model has been eliminated.

3. Materials and methods

3.1. Miscible displacements

Undisturbed soil columns were collected from two soil pedons (CR1 and CR2) located within a two ha basin in southern Costa Rica. The soil is a fine textured Ultisol (clayey kaolinitic semiactive isohyperthermic Oxyaquic Hapludult) derived from sedimentary rocks rich in mafic materials. The site has been cropped under a no-till bean-corn rotation for ten years. Undisturbed soil cores were collected at 0 to 15 cm, 20 to 40 cm, and 42 to 57 cm depths corresponding to the Ap/AB, Bt1 and Bt2 horizons, respectively, of the CR2 pedon. An additional soil core was collected at 20 to 40 cm depth corresponding to the Bt1 horizon of the CR1 pedon located at this site. Cylindrical soil columns (10.1 cm i.d.) were isolated by incrementally forcing a beveled cutting edge coupled to a polyvinyl chloride pipe over a previously carved pedestal of soil. Excess soil material at the bottom and top of the cylinders was trimmed flush and caps were secured to the ends to permit transport to the laboratory in Costa Rica. The physical parameters for each of the columns are shown in Table 1

The methods and apparatus used in the miscible displacement experiments are described in detail by Schwartz et al. (1999). Briefly, the bottom and top of each column were fitted with fritted glass plates with bubbling pressure heads ranging from -3.9 to -5.1 kPa. Contact between fritted glass plates and the soil was facilitated by placing a small amount of uniform fine-grade (#60 sieve) sand between the plate and the rough surface of the soil. Soil columns were slowly saturated with 5.0 m*M* $CaCl_2$ from the bottom porous plate prior to affixing the top plate assembly and initiating a set of displacement experiments. The inlet pressure head was controlled with a Mariotte device and the outlet pressure head was maintained by adjusting the elevation of the outflow tube. Once columns were saturated, displacement experiments were conducted under a unit hydraulic gradient at selected pressure heads of 1, -2, -5, and -10 cm H_2O (0.1, -0.2, -0.5, and -1.0 kPa) using 5.0 m*M* $CaBr_2$ as the influent solution. In some cases, greater negative pressures were applied to achieve slower water fluxes. The Br^- tracer was injected continuously only after a steady-state flux of 5.0 m*M* $CaCl_2$ had been established. Influent solution containing the Br^- tracer was continued for approximately five pore volumes or until effluent tracer concentrations were greater than 95% of the influent concentration. Once a given breakthrough run was completed for a specified head, columns were again saturated and flushed with 5.0 m*M* $CaCl_2$ solution to displace the tracer in the soil.

Table 1
Physical parameters of columns and results of the fit of the ADE to displacement experiments conducted at slow water fluxes. Only *D* and *R* were fitted for these experiments.

Column	Pedon	Horizon	ρ_b	*L*	h_{eq}	θ	q^a	*D*	*R*
			Mg m^{-3}	cm	cm H_2O	cm^3 cm^{-3}	cm h^{-1}	cm^2 h^{-1}	
1	CR2	Ap/AB	0.934	15.0	-10.0	0.510	0.63	2.45	1.50
2	CR2	Ap/AB	0.911	15.0	-10.0	0.497	0.67	3.57	1.57
3	CR2	Bt1	0.890	20.0	-10.0	0.514	1.47	5.71	2.00
4	CR2	Ap/AB	0.854	14.9	-11.0	0.636	1.11	5.68	1.16
5	CR2	Bt2	0.957	14.9	-10.0	0.547	0.82	3.01	3.04
6	CR2	Bt1	1.002	20.0	-10.0	0.554	2.17	31.1	1.53
8	CR2	Bt2	1.110	14.9	-10.0	0.568	1.58	21.7	2.89
11	CR1	Bt1	0.968	20.0	-14.0	0.618	1.17	13.8	1.40

[a] q is the volumetric flux.

The succeeding displacement experiment at the next lower head was initiated when effluent $CaBr_2$ concentrations were less than 5 μM.

Effluent from the column displacement experiments was collected over uniform time intervals corresponding to 0.1 to 0.15 pore volumes. Bromide concentrations in the effluent solution were measured using an ion-selective electrode. The ionic strengths of $CaBr_2$ standards were adjusted with $CaCl_2$ to 0.015 to match the ionic strength of the effluent exiting the columns. The soil columns were weighed at saturation and upon the completion of each displacement experiment. In addition, the oven dry weight of the soil in each column was measured after the completion of all transport studies to determine the volumetric water content at saturation and at each pressure head.

The parameters of the one-region advective dispersive equation (ADE) were identified by fitting the analytical solution of Lapidus and Amundson (1952) to effluent concentrations. For the displacement experiments conducted at the slowest flow rates corresponding to h_{eq}, the best least-squares fit of the ADE solution to measured effluent concentrations was obtained by allowing both *D* and *R* vary. Mean pore water velocity was assumed equivalent to the flux divided by the volumetric water content. Table 1 provides a summary of the results of the nonlinear least-squares estimation for the ADE (Schwartz, 1998). Solute transport at these flow rates was considered to be at or near equilibrium conditions as evidenced by the good agreement of the ADE with measured effluent concentrations and the failure of the mobile-immobile and two-region models to substantially improve predicted concentrations (Schwartz, 1998). Similar conclusions have been reached by Seyfried and Rao (1987) and Jardine et al. (1993) for unsaturated transport in undisturbed, fine-textured soils at pressure heads less than or equal to -10 cm H_2O. Parameters of the mobile-immobile region model (Parker and van Genuchten, 1984b) were fitted to dimensionless effluent concentrations with the retardation factor set equal to R_{eq}. This permitted a direct comparison between the mobile-immobile and dual-porosity models with respect to the fitted value of the mass exchange coefficient.

Values of the retardation factor exceeding unity in Table 1 result from a small amount of positive charge in soils due to the presence of goethite (7 to 11%) and an equilibrium pH in the effluent of approximately 4.6 (Schwartz, 1998). Isotherms obtained from batch adsorption experiments with bromide in a binary system with Cl^- were linear within the range of concentrations used in these displacement experiments (Schwartz et al., 1999). The retardation factor obtained from the fit of the ADE at h_{eq} (*R)* permitted the calculation of $R_{eq}(\theta)$ vis a vis Eq. (13). At pressure heads greater than h_{eq}, the ADE was fitted to effluent concentrations by allowing *D* to vary and setting the retardation factor equivalent to R_{eq}.

3.2. Micromorphology

Oriented thin sections were prepared from air dry, undisturbed clods impregnated with a polyester resin under a vacuum. The impregnating solution consisted of a 2:1 by volume mixture of polyester resin and acetone. Two g L^{-1} of fluorescent dye (UVITEX OB)** was dissolved in the acetone to improve pore visibility. Two drops of hardening agent (methyl ethyl ketone) per 100 mL solution was added to the mixture prior to impregnation. The resin was allowed to harden for eight weeks after which the samples were placed in a 60° C oven for 48 hours to cure. Vertical cross-sections of impregnated clods were cut into blocks using a diamond tipped saw blade. One side of each block was polished with a rotating lapidary unit and bonded to glass slides with epoxy resin. Bonded specimens were cut and thereafter ground to a thickness of approximately 25 μm.

3.3. Numerical solution

An implementation of the numerical method of lines (e.g. Schiesser, 1991) was used to solve the coupled system of partial differential equations. The first spatial derivatives were approximated using a five-point biased upwind method of Carver and Hinds (1978). The second derivatives were approximated using fourth-order formula obtained using Taylor series expansions. The set of ordinary differential equations resulting from the spatial discretization of Eq. (6) and (7) were integrated over time using DASSL (Differential Algebraic System Solver), a variable step-size, variable order integrator (Petzold, 1983; Brenan et al., 1989). The semi-infinite boundary condition was approximated by setting $\partial c_1(x,t)/\partial x = \partial c_2(x,t)/\partial x = 0$ at

$$x = \frac{v\,t_n}{R} + 4\cdot\sqrt{\frac{2\,D\,t_n}{R}} \qquad (15)$$

where R and D were obtained from the least-squares fit to the ADE and t_n is the time of the last concentration measurement in the effluent. Solutions for resident concentrations at the outlet, $x = L$, were transformed to flux concentrations (Parker and van Genuchten, 1984a) for each region using a fourth-order b-spline approximation of the spatial derivative (de Boor, 1978). The dimensionless flux concentration at the outlet $\bar{c}_f(L,t)$ was calculated as

$$\bar{c}_f(L,t) = \frac{v_1\,\theta_1\,c_{f1}(L,t) + v_2\,\theta_2\,c_{f2}(L,t)}{v_1\,\theta_1 + v_2\,\theta_2} \qquad (16)$$

where c_{f1} and c_{f2} are the flux concentrations in the macropore and matrix regions respectively.

3.4. Nonlinear least-squares estimation

Modeled dimensionless flux concentrations at the outlet $\bar{c}_f(L,t)$ were fitted to dimensionless effluent concentrations $[C_f(L,t) - C_f(L,0)] / [C_0 - C_f(L,0)]$ using an adaptive, model-trust region method of nonlinear, least-squares parameter optimization (Dennis et al., 1981; Dennis and Schnabel, 1983). Derivatives of the two-region dimensionless flux solution with respect to each fitting parameter were calculated using forward differencing. Iterations of the nonlinear least-squares estimation procedure were continued until both the maximum scaled relative change in the parameters and the ratio of forecasted change in the residual sum of squares were less than 1×10^{-6}. Combinations of four or fewer model parameters (D_1, D_2, R_1, ε, v_2, and θ_2) were fitted to breakthrough curves to identify the parameter sets that yielded convergence and the lowest sum of squared residuals (SSR). The coefficient R_2 was always redefined as a function of R_1 and $R_{eq}(\theta)$ to satisfy Eq. (14) corresponding a constant $R_{eq}(\theta)$ for a given water content and hence a constant K_d for a given soil column. When v_2 was fitted, a constant flux was maintained by resetting $v_1 = (q - v_2\cdot\theta_2)/\theta_1$ where q is total mass flux. Hence the solute flux contributed by each region was permitted to change. Starting values of parameters were selected based on the fit of the ADE at both pressure heads and previous fits of the dual-porosity model. At least three sets of parameter starting values were used for each estimation problem to ensure that the optimization routine converged to a global minimum. In a few cases, convergence problems were encountered for three and four parameter fits. This was attributed to model overspecification as indicated by the failure of SSR to change significantly (1×10^{-6}) despite large changes in parameter estimates.

** The mention of trade or manufacturer names is made for information only and does not imply an endorsement, recommendation, or exclusion by USDA-Agricultural Research Service.

Table 2
Measured and estimated parameters for the constrained fit of the dual-porosity model to effluent concentrations of displacement experiments (Values in parenthesis signify the 95% confidence interval as calculated from asymptotic standard errors.)

Column	Pedon	Horizon	h	θ_1	θ_2	v_1	v_2	D_1	D_2 [a]	R_1 [b]	ε	R_2 [b]	f	SSR
			(cm)	(cm^3 cm^-	(cm^3 cm^-	(cm h^{-1})	(cm h^{-1})	(cm^2 h^{-1})	(cm^2 h^{-1})		(h^{-1})			$\times10^{-2}$
1	CR2	Ap/AB	1.0	0.108	0.510	438	1.23	586	586	3.36	23.3	1.00	1.00	13.114
								(218)			(7.0)			
1	CR2	Ap/AB	-2.0	0.044	0.510	225	1.23	101	101	6.79	45.8	1.00	1.00	0.855
								(15)			(13.6)			
2	CR2	Ap/AB	1.0	0.128	0.497	892	1.34	1972	1972	3.23	22.8	1.00	1.00	1.577
								(273)			(3.0)			
2	CR2	Ap/AB	-2.0	0.045	0.497	484	1.34	170	170	7.33	96.2	1.00	1.00	0.928
								(42)			(37.9)			
3	CR2	Bt1	1.0	0.142	0.514	1197	2.87	14787	14787	3.65	4.48	1.27	0.73	1.539
								(1769)		(0.16)	(1.48)			
3	CR2	Bt1	-2.0	0.031	0.514	235	2.87	87.8	87.8	17.79	51.0	1.00	1.00	3.235
								(7.4)			(23.3)			
4	CR2	Ap/AB	1.0	0.044	0.636	1467	1.75	1493	1493	3.33	884	1.00	1.00	17.708
								(2021)			(13893)			
5	CR2	Bt2	1.0	0.041	0.547	159	1.49	1986	390	21.27	0.025	1.51	0.75	0.774
								(116)	(305)	(1.36)				
5	CR2	Bt2	-2.0	0.024	0.547	171	1.49	1541	15.0	43.13	0.025	1.23	0.89	0.078
								(694)	(17.7)	(13.21)				
5	CR2	Bt2	-5.0	0.017	0.547	126	1.49	376	52.8	50.42	0.025	1.52	0.74	0.383
								(21)	(7.7)	(1.24)				
6	CR2	Bt1	1.0	0.056	0.554	799	3.93	5532	5532	6.24	7.11	1.00	1.00	0.932
								(462)			(1.06)			
6	CR2	Bt1	-3.0	0.033	0.554	657	3.93	1419	1419	9.79	33.7	1.00	1.00	10.500
								(370)			(19.2)			
8	CR2	Bt2	1.0	0.006	0.568	1439	2.79	8684	226	35.77	0.025	2.53	0.19	2.615
								(2534)	(73)	(3.17)				
8	CR2	Bt2	-2.0	0.003	0.568	710	2.79	3807	77.1	59.97	0.025	2.54	0.19	1.658
								(1465)	(13.8)	(7.37)				
8	CR2	Bt2	-5.0	0.001	0.568	496	2.79	1238	76.7	137.06	0.025	2.69	0.11	0.389
								(405)	(4.7)	(16.90)				
11	CR1	Bt1	1.0	0.019	0.618	365	1.89	4757	102	13.69	0.025	1.01	0.97	1.423
								(912)	(33)	(1.10)				
11	CR1	Bt1	-10.0	0.013	0.618	211	1.89	953	15.1	20.69	0.025	1.00	1.00	0.871
								(113)	(1.8)					

[a] Matrix dispersion coefficients (D_2) without a confidence interval were set equal to D_1 for the least-squares fit.
[b] R_1 was fit such that the values of R_1 and R_2 always satisfied Eq. (14) with $R_{eq}(\theta)$ defined by Eq. (13).

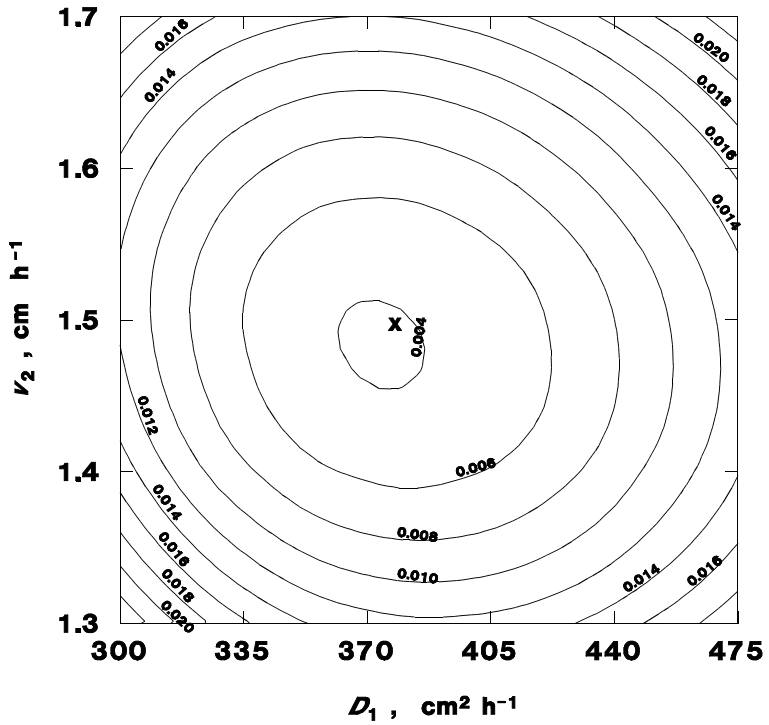

Fig. 1. Response surface of the sum of squared residuals in the D_1 - v_2 parameter plane for the displacement experiment of column 5 at h = -5 cm H_2O. The fitted values of the remaining model parameters shown in Table 2 were used to calculate the solutions. The location of the best fit solution is marked with an "**X**" at v_2 = 1.49 cm h^{-1} and D_1 = 376 cm^2 h^{-1}.

The fit of the dual-porosity model to observed flux concentrations was constrained to realistic parameter values. Accordingly, ε, D_1, D_2, v_1, and v_2 were limited to values greater than zero and R_1 and R_2 were limited to values greater than unity. A final constraint was imposed such that D_2 could not exceed the fitted value of D_1. This requirement is based upon the reasoning that a tracer moving through the matrix initially free of the tracer should not appear at the exit boundary in this region at higher resident concentrations than the macropore region.

4. Results and discussion

4.1. Model fits to effluent concentrations

In general, least-squares fits obtained using sets of parameters that included v_2 did not significantly decrease (by 5%) the sum of squared residuals (SSR). In those cases where significant improvement of the SSR was obtained, v_2 converged to unrealistically small or large values. These difficulties were not resolved by fixing R_1 to a constant value. Figures 1 and 2 represent the response surface exhibited by the SSR within the D_1 - v_2 and R_1 - v_2 parameter space for the column 5 displacement experiment at h = -5 cm H_2O. These plots demonstrate why a shift in the value of v_2 did not result in significant improvements in the SSR. Moreover, the long narrow valley exhibited by the response surface in Figure 2 suggests that v_2 is difficult to identify when R_1 is also unknown. This also explains why large standard errors were often obtained concomitant with low SSR across a wide range in velocities for parameter fits that included v_2. Thus, treating v_2 as a known parameter increased the identifiability of the remaining parameters, especially when R_1 (or R_2) was unknown. Since adsorption within a single pore region cannot be measured, the estimation of v_1 and v_2 from the measurements of water flux and water content at two different pressure heads was the most suitable method

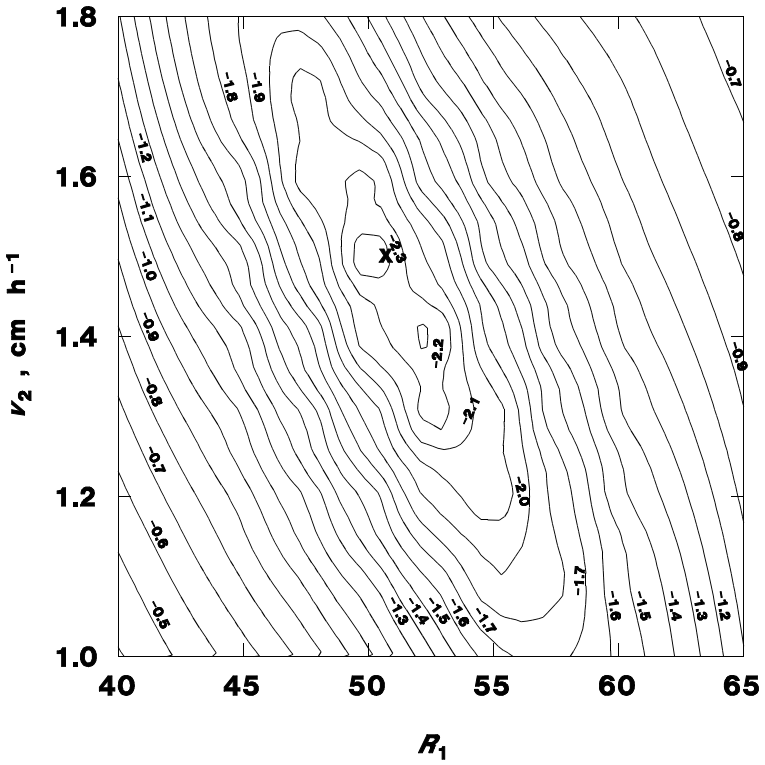

Fig. 2. Response surface of the log of sum of squared residuals in the R_1 - v_2 parameter plane for the displacement experiment of column 5 at h = -5 cm H_2O. The fitted values of the remaining model parameters shown in Table 2 were used to calculate the solutions. The location of the best fit solution is marked with an "**X**" at v_2 = 1.49 cm h^{-1} and R_1 = 50.4.

for ascribing solute flux to each region. Accordingly, all subsequent discussions regarding the dual-porosity model pertain to least-squares fits with velocity in each region fixed.

For nearly all of the initial least-squares fits where D_1, D_2, R_1, and ε were permitted to vary, at least one parameter was outside of the boundaries identified above which delineate a physically acceptable solution domain. The four-parameter fits of the dual-porosity model to effluent concentrations were characterized by two distinct groups: (1) those fits in which ε converged to negative values and (2) those fits in which R_2 converged to values less than one and frequently D_2 converged to values greater than D_1. The above differences in the least-squares fits were *consistently* associated with the soil horizon. The Bt2 horizon of the CR2 pedon and the Bt1 horizon of the CR1 pedon consistently exhibited fits corresponding to ε converging to negative values. In contrast, the Ap/AB and Bt1 horizons of the CR2 pedon exhibited fits corresponding to convergence of R_2 less than unity and D_2 converging to values greater than D_1.

For the Bt2 horizon of the CR2 pedon and the Bt1 horizon of the CR1 pedon, a solution satisfying a nonnegative value of ε was obtained by fitting the dual-porosity model with a small first-order mass transfer coefficient estimated as

$$\varepsilon = \frac{\beta}{a^2} D_a \tag{17}$$

where D_a is the effective diffusion coefficient (L^2 T^{-1}), β is a dimensionless geometry-dependent coefficient, and a is an effective radius of aggregates (Gerke and van Genuchten, 1996). For the subsoils a was set to 3 cm, β was approximated as 3 for rectangular slabs (Gerke and van Genuchten, 1993b), and D_a was

estimated using the molecular diffusion coefficient of Br^- in water (0.075 $cm^2\ h^{-1}$).

Solutions satisfying the constraints on R_1, R_2, and D_2 for the Ap/AB and Bt1 horizons of the CR2 pedon were obtained by 1) setting R_2 to unity and R_1 as a function of R_{eq} and R_2 given in Eq. (14) and/or 2) setting D_2 equivalent to D_1 and allowing both to vary as a fitted parameter. Besides delineating an acceptable solution domain, the second strategy also eliminated the large negative covariances exhibited between D_1 and ε. The solution of the dual-porosity model was quite insensitive to large variations in D_2 likely due to the fact that the matrix region accounts for only a small proportion of the total effluent flux. Fitting the dual-porosity model with D_2 set equal to D_1 provided only a slightly better SSR than setting D_2 equal to the dispersion coefficient obtained from the ADE fit to the matrix region in isolation, despite a change in the dispersion coefficient by up to two order in magnitude. A lower SSR could often be obtained by letting D_2 greatly exceed (e.g. by an order of one magnitude) D_1. Dispersion coefficients of the slowly mobile region exceeding those of the regions with greater mobility was also reported by Gwo et al. (1995). For this study, while letting D_2 exceed D_1 yielded lower SSR, residuals and estimated studentized residuals at very early times were larger than those obtained when D_2 was held equal to D_1 in all but one case. This supports the presumption that to arrive at realistic values of concentrations at early times, D_2 should be no greater than D_1.

A summary of the results of the best least-squares fits of the dual-porosity model to effluent concentrations using the constraints discussed above is provided in Table 2. These results are compared with the best fit ADE solution with $R = R_{eq}(\theta)$ in Fig. 3 for several horizons. In every case, the two and three-parameter fit of the dual-porosity model had a lower residual standard deviation than the one-parameter ADE fit. In one instance, however, (column 4 at a pressure head of 1 cm H_2O) the fit was overspecified as judged by the magnitude of the confidence intervals of all parameters.

4.2. Analysis of fitted parameters

The nonlinear least-squares fit of the dual-porosity model to measured effluent concentrations yielded column Péclet numbers ($v\ L\ /\ D$) ranging from 1 to 50 for the macropore region and from .004 to 3 for the matrix region. As discussed by van Genuchten and Parker (1984), these Péclet numbers are small enough to produce differences in fitted coefficients as a result of the choice in boundary conditions used in the numerical solution. The dispersion coefficient in the macropore region, D_1, exhibited a log linear relationship with mean pore water velocity in this region (Fig. 4). The relationship of D_1 with v_1 differed substantially between horizons and in some cases among horizons. The variability of the dispersivity relationship exhibited in Fig. 4 calls into the question the validity of using v_1 to estimate D_1 for use in the dual-porosity model. For transient modeling applications, the predictability of D_1 is of major importance and the inability to obtain reliable estimates will limit the usefulness of the model in a predictive mode.

A principle difficulty with the least-squares fit of the dual-porosity model for the Ap/AB and Bt1 horizons of the CR2 pedon was the tendency of the fraction of adsorption sites in equilibrium with solute concentration in macropores (f) to exceed unity. For these horizons f was set to unity to obtain a physically acceptable solution that corresponds to no solute adsorption in the matrix region. This signifies that all adsorption sites were in equilibrium with the solute concentration in the macropore region despite the lack of equilibrium of solution concentrations between regions. Such a condition is clearly not realistic considering that the matrix region comprises a considerably greater volume than the macropore region. This outcome may be a result of the model assumption of a single bulk density for both regions and a spatially invariable distribution coefficient. Large fitted values of f may also result from the presumption of complete mixing within the macropore region. This is demonstrated by comparing solutions obtained for a range of f (Fig. 5) and noting that early effluent concentrations are relatively sensitive to this parameter. A small f equivalent to $\theta_1/(\theta_1+\theta_2)$ overestimates early concentrations and underestimates late concentrations. It is possible that limited mixing between individual macropores generated a non-normally distributed solute velocity within this region. As a result, the retardation factor in this region may have been fitted to large values to offset large concentrations predicted at early times by the model.

The convergence of the exchange coefficient, ε, to values less than zero likely resulted from the inability

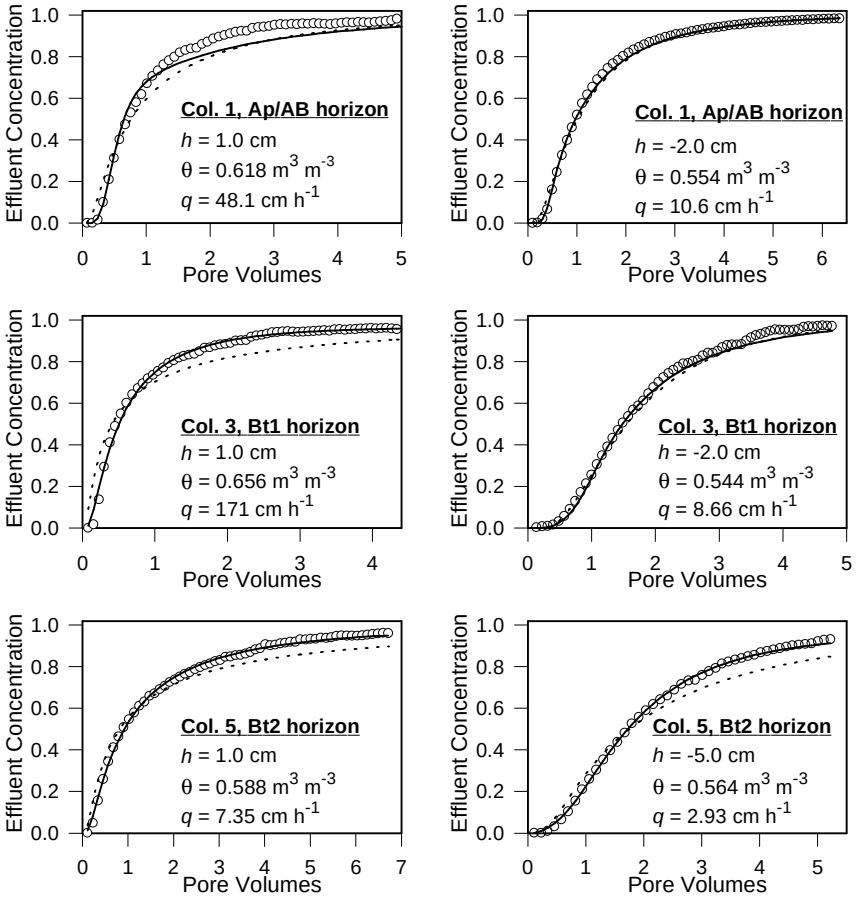

Fig. 3. Comparison of measured (○) with predicted (–) relative effluent concentrations of the dual-porosity model for the Ap/AB, Bt1, and Bt2 horizons of the CR2 pedon over a range of soil water fluxes (q) at prescribed pressure heads (h). Dotted line is best fit ADE solution with R set equal to $R_{eq}(\theta)$.

of the linear mass exchange term to describe diffusion into aggregates at early times. Figure 6 shows the variation of the fitted mass transfer coefficient, ε, obtained by fitting the dual-porosity model to effluent concentrations over short time intervals with D_2, R_1, and R_2 fixed to values shown in Table 2 for column 5 at a pressure head of 1 cm H_2O. Thus the fitted value of ε at $t = 0.40$ represents the fit of the dual-porosity model to effluent concentration measurements obtained from $t = 0.13$ (the first measurement) to $t = 0.67$. The fitted value of D_1 for these five least-squares fits averaged 1851 $cm^2\ h^{-1}$ and does not differ substantially from the fitted value for the entire breakthrough curve (1986 $cm^2\ h^{-1}$). Based on Fig. 6, it is evident that the magnitude of the mass transfer coefficient decreases with time. This result has also been demonstrated by Rao et al. (1980) by matching the analytical results of a model explicitly accounting for transverse diffusion with the solution of the mobile-immobile model. As a consequence of the nonlinearity of ε with concentration differences, mass exchange between regions is underestimated by the dual-porosity model at early times. Apparently, this discrepancy between model assumptions and actual physical processes related to solute exchange between regions caused ε to converge to slightly negative values that yielded lower SSR's rather than convergence to large values associated with local equilibrium conditions. Although the time dependent relationship

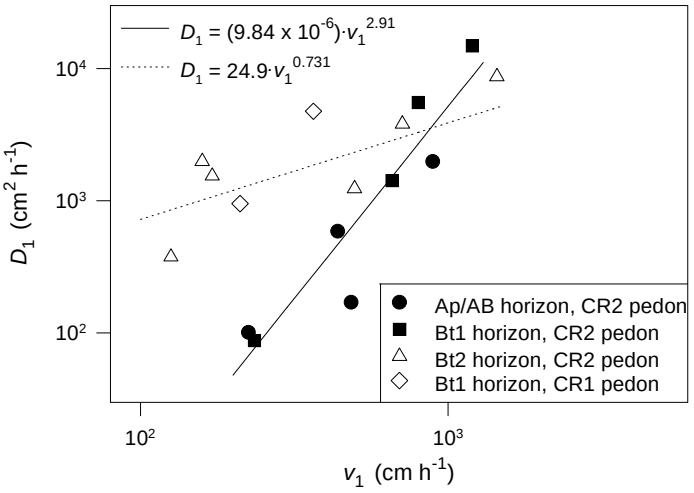

Fig. 4. Influence of the mean pore water velocity in the macropore region on the dispersion coefficient obtained from the least-squares fit of the dual-porosity model for several soil horizons.

$\ln(\varepsilon) = \beta_0 + \beta_1 t$ was found to provide improved fits (data not shown) and led to nonnegative values of the exchange coefficient, such an expression further increases the number of parameters that must be estimated and, in this respect, is undesirable.

The variation of $1/\varepsilon$ as a function of the longitudinal interaction time scale expressed as $D_1 / (v_1 - v_2)^2$ assuming $D_2 = D_1$ for the dual-porosity model represents the degree of interaction between regions due to the averaging effects of the local flow variations (Li et al., 1994). The relatively strong relationship (i.e. large slope) between $1/\varepsilon$ and the longitudinal interaction time scale for the Ap/AB horizon and Bt1 horizon of the CR2 pedon (Fig. 7) signifies that the timescale for transverse interaction via diffusive transport was extremely rapid. Clearly this scenario can result when the transverse length scale corresponding, for instance, to an effective aggregate diameter is insignificant. An

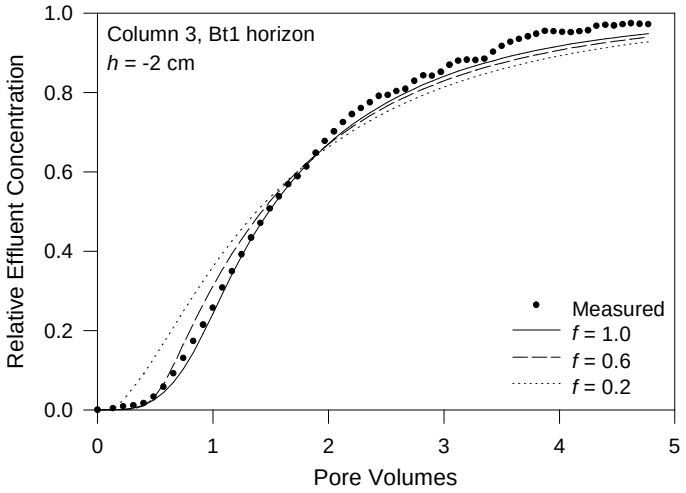

Fig. 5. Sensitivity of the solution of the dual-porosity model with respect to the fraction of adsorption sites in equilibrium with the solute concentrations in macropores.

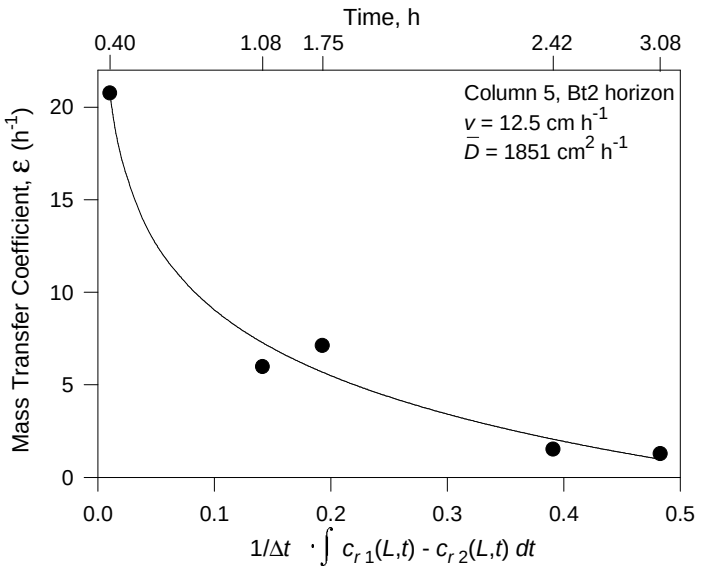

Fig. 6. Time-dependency of the mass transfer coefficient and its correspondence with differences in concentration as assessed by fits of the dual-porosity model to different time intervals of the breakthrough curve obtained for column 5 at a pressure head of 1 cm H_2O. The *x*-axis denotes the average resident concentration at $x = L$ obtained by integrating over each respective time interval.

exponent close to unity (1.14) for the trend exhibited in Fig. 7 corresponds closely with the hypothesis by Li et al. (1994) that $1/\varepsilon$ should be proportional to $D_1 / (v_1 - v_2)^2$. Obviously, since the value of ε was fixed for the least-squares fits of the dual-porosity model involving columns obtained from the Bt2 horizon and the Bt1 horizon of the CR1 horizon, the relative importance of the longitudinal time scale cannot be assessed for these horizons. However, the fact that an unvarying value of ε yielded acceptable least-squares fits for each column across a range in velocities with little change in water content suggests that transverse interactions via diffusive transport dominate solute transfers between regions for these horizons.

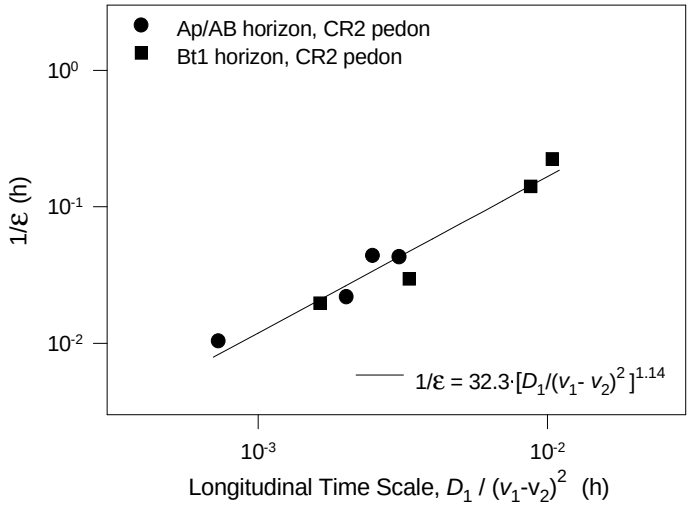

Fig. 7. Variation of the inverse of the mass transfer coefficient with respect to the longitudinal interaction time scale.

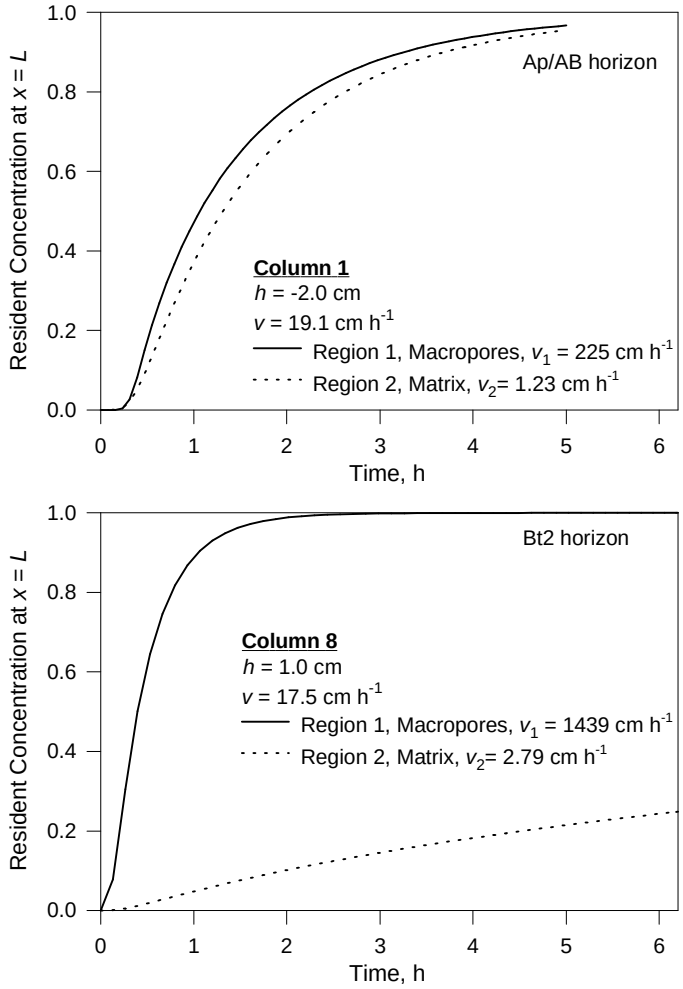

Fig. 8. Resident concentrations in the macropore and matrix regions predicted by the fit of the dual-porosity model to breakthrough curves for the Ap/AB and Bt2 horizons of the CR2 pedon.

4.3. Significance of model results

The model predictions of large differences in transport between the surface (Ap/AB) and Bt2 horizons of the CR2 pedon as evidenced by the magnitude of ε is not readily apparent in Fig. 3. The differences, however, are evident when predicted resident concentrations in each region are plotted as a function of time (Fig. 8). Obviously, the resident concentrations within the matrix region of the Bt2 horizon lag considerably behind the macropore concentrations. In contrast, the model fit obtained for the Ap/AB horizon at approximately the same pore water velocity demonstrates that both regions are nearly at equilibrium. These interpretations essentially reflect the contrasting structures exhibited by the soil near the surface and in the lower Bt horizons. Thin section micrographs shown in Fig. 9 illustrate obvious structural differences between the Ap and Bt2 horizons. The fabric of the Ap horizon consisted of a discontinuous S-matrix dissected by a highly interconnected pore network. In contrast, micrographs of the Bt2 horizon were characterized by more extensive regions of plasma with fewer visible pores. Since a larger mass exchange coefficient corresponds to shorter travel distances between macropores and intra-

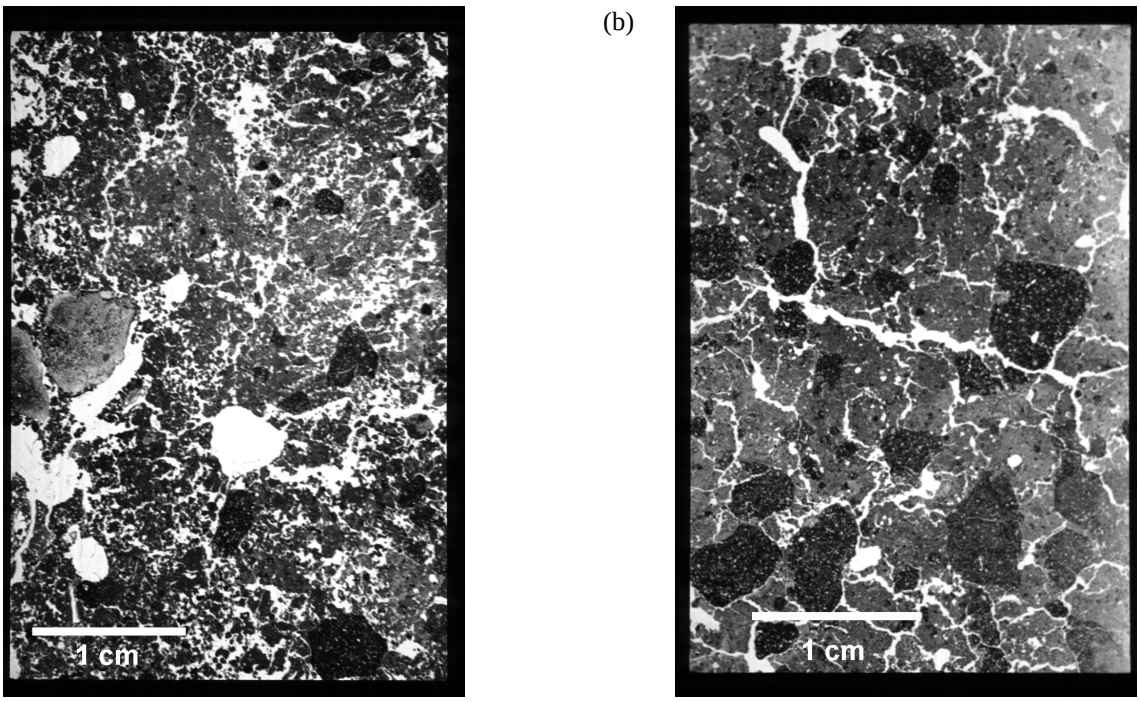

Fig. 9. Thin-sections of peds obtained from the a) Ap and b) Bt2 horizons of the CR2 pedon.

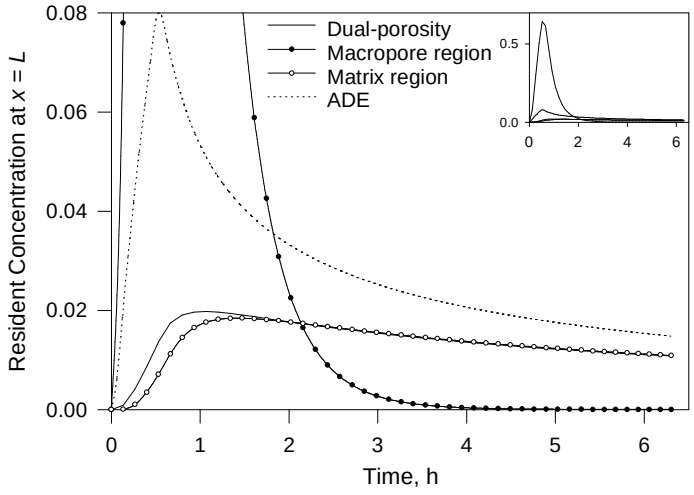

Fig. 10. Simulated resident concentrations at $x = L$ for column 8 at a pressure head of 1 cm H_2O resulting from a Br^- pulse of duration 0.5 hours. Resident concentrations calculated for the dual-porosity model are volume averaged between regions. Inset graph is identical except that the *y*-axis is modified to show the resident concentrations for the macropore region.

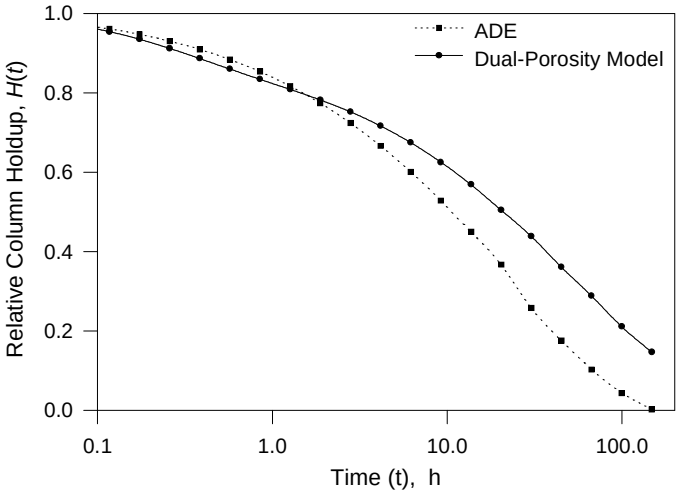

Fig. 11. Relative column holdup as a function of time calculated from the best fit ADE and dual-porosity model parameters obtained from the column 8 displacement experiment at a pressure head of 1 cm H_2O.

aggregate regions, model predictions of the exchange coefficient for these horizons correspond well to the degree to which continuous pores permeate the matrices as illustrated in the thin sections. Such a distinction between horizons was not evident for fits of the mobile-immobile model (Schwartz, 1998). For example, the fitted value of the mass transfer term, α, for the Ap/AB horizon ranged from 0.019 to 1.072 h^{-1} and intersected the range obtained for the Bt2 horizon (0.016 - 0.035 h^{-1}). In contrast, the equivalent term for the dual-porosity model $(\varepsilon\theta_1\theta_2)/(\theta_1+\theta_2)$ ranged from 1.86 to 3.97 h^{-1} for the Ap/AB horizon and converged to negative values for the Bt2 horizon. In this respect, the dual-porosity model led to a better differentiation of transport processes that corresponded to observed structural differences in the soils.

The mean residence time μ_1 of a solute pulse for the dual-porosity model was estimated as

$$\mu_1 = \int_0^t 1 - c_f(L,\tau)\, d\tau \qquad (18)$$

using very large t and found to approach $L\, R_{eq} / v$, the theoretical mean residence time of the ADE. Hence, for the dual-porosity model with semi-infinite boundaries, physical nonequilibrium does not influence the mean breakthrough time of the solute pulse. This agrees with the analytical results of Valocchi (1985) for physical and chemical nonequilibrium models with only one mobile region. The distinction between the ADE and the dual-porosity model is contained within the 2nd and higher moments of the residence time distribution function which is manifested by the degree of spreading, tailing, and peakedness. Figure 10 shows the simulated resident concentrations at the exit boundary for column 8 at h = 1 cm H_2O resulting from a pulse of Br^- of duration 0.5 hours. Clearly, the solute flux in the matrix region, which comprises at least 99% of the soil water for this column, is relatively insensitive to changes in solute concentration in the macropore region. As a result, very little solute is exchanged between regions and volume averaged resident concentrations in the column are less than that predicted by the advective-dispersive equation. Similarly, solute contained within the matrix region will have extremely long residence times. This is demonstrated by plotting relative column holdup $H(t)$ over time t which reflects the proportion of solute in the column at time t with respect to the amount initially present at t = 0 and calculated as

$$H(t) = 1 - \frac{1}{\mu_1} \cdot \left[t - \int_0^t c_f(L,\tau)\, d\tau \right] \qquad (19)$$

The plot of relative column holdup for effluent concentrations is simulated in Fig. 11 for the displacement experiment for column 8 at a pressure head of 1 cm H_2O using the parameters obtained from the best fit ADE and dual-porosity model. At early times it is evident that relative holdup predicted by the

dual-porosity model is slightly less than that predicted by the ADE. However at $t > 1$ hour, relative column holdup predicted by the dual-porosity model is significantly greater than the ADE prediction indicating the extremely slow rate of solute transfer from the matrix region to the highly mobile macropore region.

5. Conclusions

In this study, the parameters of the dual-porosity model were fitted to column effluent concentrations to evaluate reactive, nonequilibrium transport in a fine-textured soil. Acceptable fits of the dual-porosity model with lower residual standard deviations than the ADE could be obtained while holding the bulk distribution coefficient of the soil constant and constraining ε, f, and D_1 to realistic values. The magnitude of the fitted mass exchange coefficient corresponded, in a qualitative sense, to observed soil structural differences. Such a correspondence between the exchange co
efficient and soil structure was not obtained for the fits of the mobile-immobile model. This outcome may be partly attributed to the independent estimation of pore water velocity in each region of the dual-porosity model using a pair of displacement experiments. The principal difficulties of the application of the dual-porosity model to solute transport in these soils related to the nonlinear behavior of the mass exchange term at early times and the tendency fitted solutions to predict that nearly all adsorption sites were in equilibrium with the solute concentration in the macropore region despite the fact that solute concentrations within the two regions were not in equilibrium.

The successful use of dual-porosity model in a predictive mode will require the estimation of D_1, f, ε, and less importantly D_2. Based on the results of this study, difficulties in obtaining satisfactory estimates of D_1, D_2 and f are anticipated. Such difficulties are likely to be magnified considering that these parameters must be estimated over a range of water contents and associated pore water velocities for each region in order to apply the non-steady-state model to actual field conditions. The fitted mass exchange coefficient may represent a lumped process resulting from the combined effects of intra-aggregate diffusion and local flow variations. When there is limited interaction between regions, the mass transfer coefficient should be estimated by matching model solutions with diffusion models using specified ped geometries or, better yet, by measuring the rate of diffusion of solute into soil peds through a known surface area. Presently, it does not seem possible to obtain independent estimates of these parameters when there is a significant amount of interaction between regions. However, this represents a scenario that may be adequately described by one-region transport models. For the soils used in this study, the dual-porosity model provided a more consistent description of solute transport in the subsoil horizons that possessed matrix regions largely isolated from a highly mobile pore network. Such an outcome is anticipated since the conceptualization implied by the dual-porosity model corresponds more closely to porous media in which there exist two distinct regions which behave independently except for exchanges.

Acknowledgments

We are indebted to Carlos Cervantes of the Universidad Nacional for support of research activities in Costa Rica. Special thanks is extended to Richard Drees for assistance in the preparation of thin sections. The comments and suggestions of Horst Gerke and an anonymous reviewer are gratefully acknowledged. This work was supported in part by the Soil Management Collaborative Research Support Program (USAID Grant No. DAN-1311-G-SS-6018-00).

References

Barenblatt, G.I., Zheltov, Iu.P., and Kochina,.I.N., 1960. Basic concepts in the theory of seepage of homogeneous liquids in fissured rocks. Prikl. Mat. Mekh., 24, 852-864.

Brenan, K.E., Campbell, S.L., and Petzold., L.R., 1989. Numerical Solution of Initial-Value Problems in Differential-Algebraic Equations. Elsevier Sci. Publ. Co., Inc., New York, N.Y.

Carver, M.B. and Hinds, H.W. 1978. The method of lines and the advection equation. Simulation, 31, 59-69.

Coats, K.H. and Smith, B.D., 1964. Dead-end pore volume and dispersion in porous media. Soc. Pet. Eng. J., 4, 73-84.

de Boor, C., 1978. A Practical Guide to Splines. Springer-Verlag, New York, NY.

Dennis, J.E.,. Gay, D.M, and Welsch, R.E., 1981. An adaptive nonlinear least-squares algorithm. ACM Trans. Math. Softw., 7, 348-368.

Dennis, J.E. and Schnabel, R.B., 1983. Numerical Methods for Unconstrained Optimization and Nonlinear Equations. Prentice-Hall, Inc., Englewood Cliffs, NJ.

Elrick, D.E. and French, L.K., 1966. Miscible displacement patterns on disturbed and undisturbed soil cores. Soil Sci. Soc. Am. Proc., 30, 153-156.

Gerke, H.H. and van Genuchten, M.Th., 1993a. A dual-porosity model for simulating the preferential movement of water and solutes in structured porous media. Water Resour. Res., 29, 305-319.

Gerke, H.H. and van Genuchten, M.Th., 1993b. Evaluation of a first-order water transfer term for variably saturated dual-porosity flow models. Water Resour. Res., 29, 1225-1238.

Gerke, H.H. and van Genuchten, M.Th., 1996. Macroscopic representation of structural geometry for simulating water and solute movement in dual-porosity media. Adv. Water Resour., 19, 343-357.

Gwo, J.P., Jardine, P.M., Wilson, G.V., and Yeh, G.T., 1995. A multiple-pore-region concept to modeling mass transfer in subsurface media. J. Hydrol., 164, 217-237.

Hutson, J.L. and Wagenet, R.J. 1995. A multiregion model describing water flow and solute transport in heterogeneous soils. Soil Sci. Soc. Am. J., 59, 743-751.

Jardine, P.M., Jacobs, G.K., and Wilson, G.V., 1993. Unsaturated transport processes in undisturbed heterogeneous porous media: I. Inorganic contaminants. Soil Sci. Soc. Am. J., 57, 945-953.

Lapidus, L. and Amundson, N.R., 1952. Mathematics of adsorption in beds. VI. The effect of longitudinal diffusion in ion exchange and chromatographic columns. J. Phys. Chem., 56, 984-988.

Li, L., Barry, D.A.,Culligan-Hensley, P.J., and Bajracharya, K., 1994. Mass transfer in soils with local stratification of hydraulic conductivity. Water Resour. Res., 30, 2891-2900.

Ma, L. and Selim, H.M., 1995. Transport of a nonreactive solute in soils: A two-flow domain approach. Soil Sci., 159, 224-234.

Parker, J.C. and van Genuchten, M.Th., 1984a. Flux-averaged and volume-averaged concentrations in continuum approaches to solute transport. Water Resour. Res., 20, 866-872.

Parker, J.C. and van Genuchten, M.Th., 1984b. Determining Transport Parameters from Laboratory and Field Tracer Experiments. Va. Agric. Exp. Stn. Bull. 84-3, Virginia Agricultural Experiment Station, Blacksburg, VA.

Petzold, L., 1983. A description of DASSL: a differential/algebraic system solver. In: R.S. Stepleman (Editor) IMACS Transactions on Scientific Computation, North-Holland, Amsterdam.

Rao, P.S.C., Jessup, R.E., Rolston, D.E., Davidson, J.M., and Kilcrease, D.P., 1980. Experimental and mathematical description of nonadsorbed solute transfer by diffusion in spherical aggregates. Soil Sci. Soc. Am. J., 44, 684-688.

Ray, C., Boast, C.W., Ellsworth, T.R., and Valocchi, A.J., 1996. Simulation of the impact of agricultural management practices on chemical transport in macroporous soils. Trans. ASAE, 39, 1697-1707.

Ray, C., Ellsworth, T.R., Valocchi, A.J., and Boast, C.W., 1997. An improved dual porosity model for chemical transport in macroporous soils. J. Hydrol., 193, 270-292.

Schiesser, W.E., 1991. The Numerical Method of Lines -- Integration of Partial Differential Equations. Academic Press, Inc., San Diego, CA.

Schwartz, R.C. 1998. Reactive transport of tracers in a fine-textured Ultisol. Ph.D. thesis. Texas A&M University, College Station, TX.

Schwartz, R.C., McInnes, K.J., Juo, A.S.R., Reddell, D.L., and Wilding, L.P., 1999. Boundary effects upon solute transport in finite soil columns. Water Resour. Res., 35, 671-681.

Seyfried, M.S. and Rao, P.S.C., 1987. Solute transport in undisturbed columns of an aggregated tropical soil: preferential flow effects. Soil Sci. Soc. Am. J., 51, 1434-1444.

Skopp, J., Gardner, W.R., and Tyler, E.J., 1981. Solute movement in structured soils: two-region model with small interaction. Soil Sci. Soc. Am. J., 45, 837-842.

Valocchi, A., 1985. Validity of the local equilibrium assumption for modeling sorbing solute transport through homogeneous soils. Water Resour. Res., 21, 808-820.

van Genuchten, M.Th. and Parker, J.C., 1984. Boundary conditions for displacement experiments through short laboratory soil columns. Soil Sci. Soc. Am. J., 48, 703-708.

van Genuchten, M. Th. and Wierenga, P.J.1976. Mass transfer studies in sorbing porous media: analytical solutions. Soil Sci. Soc. Am. J., 40, 473-480.

Warren, J. and Root, P., 1963. The behavior of naturally fractured reservoirs. Trans. AIME, 228, 245-255.